Supplement of Atmos. Chem. Phys., 24, 10513–10529, 2024
https://doi.org/10.5194/acp-24-10513-2024-supplement

Atmospheric Chemistry and Physics
Open Access

Supplement of

Observational and model evidence for a prominent stratospheric influence on variability in tropospheric nitrous oxide

Cynthia D. Nevison et al.

Correspondence to: Cynthia D. Nevison (cynthia.nevison@colorado.edu)

S1. Methodology for evaluating statistical significance in correlation analysis

The statistical significance of the correlation coefficients presented in Sections 3.2-3.3 can be assessed by testing the hypothesis that the true R is significantly different from 0. This involves comparing the calculated R values to critical R values determined from a t-table (see Box 15.3 of *Sokal and Rohlf*, 1981). This test is a function of significance level and degrees of freedom ν (ν = N-2). The PLST correlations were based in all cases on N = 21 ± 1 data points, a single value for each year in the time series. The statistics for the QBO and ENSO correlations were based on monthly mean time series and therefore have a variable N due to the autocorrelation that is introduced in part by the 12-month running mean used to deseasonalize N_2O to compute the AGR. To account for autocorrelation in each time series, an effective N ($N_{eff} = N/\kappa$) was used to calculate ν, where κ is the integrated area of the autocorrelation vs. lag curve centered around 0 lag for which the autocorrelation coefficient $\rho > 0.1$ (*Carlin and Louis*, 2000, p. 171). The autocorrelation for the QBO and ENSO indices was computed in the same way and the smaller of the N_{eff} values (for N_2O AGR and the correlate index), was used. For NH and SH N_2O AGR vs. QBO correlations, N_{eff} was 21 and 24, respectively, for NOAA and 14 and 19, respectively, for GEOSCCM. For NH, SH and global NOAA N_2O AGR vs. ENSO correlations, the values of N_{eff} were ~ 14, 10, and 13, respectively. The calculated N_{eff} values were compared to T tables at 99%, 95% and 90% confidence to determine critical R values (*Sokal and Rohlf*, 1981]. The latter were compared to the N_2O AGR vs. correlate index to classify the p value into 4 categories: $p > 0.10$, $0.10 > p > 0.05$, $p < 0.05$ (but > 0.01), and $p < 0.01$.

S2. Why is QBO positively correlated to the N_2O atmospheric growth rate anomaly in the southern hemisphere?

The QBO is the primary mode of variability governing the amount of N_2O that is transported from the tropical lower stratosphere into the middle and upper tropical stratosphere, the region of peak photochemical destruction (*Baldwin et al.*, 2001; *Prather et al.*, 2015; *Ruiz et al.,* 2021). Photochemical destruction is highest when QBO winds at higher altitudes (~30 hPa and above) are in the westerly (positive) phase and lower altitude QBO winds are in the easterly (negative) phase. This configuration is associated with increased vertical upwelling in the tropical lower stratosphere, which transports more N_2O to its peak loss region around 32 km (*Strahan et al.*, 2021; *Ruiz et al.*, 2021).

In addition to the primary vertical circulation, the QBO has an associated secondary or meridional circulation, which in the SH involves transport of photochemically-depleted tropical air into the subtropical middle stratosphere followed by planetary wave-driven mixing, which homogenizes this air over a broad area known as the "surf zone" (*Strahan et al.*, 2015). The surf zone extends from about 30 hPa to 10 hPa in altitude and 15-70º S in latitude. Paradoxically, in the positive QBO phase in the upper stratosphere, when the N_2O photochemical loss is at its peak, relatively less N_2O-depleted air enters the subtropical surf zone, due to the upward/clockwise flow of the secondary QBO circulation (*Strahan et al.*, 2015).

N_2O-depleted air in the surf zone (set by the QBO) subsequently is mixed into the polar region during the late spring breakup of the Antarctic polar vortex and summer-to-fall SH vortex development. The N_2O anomaly is then set into the Antarctic region as the polar vortex forms in the fall. The vortex-trapped N_2O anomaly undergoes diabatic descent, driven by the BDC and in isolation from mixing with lower latitudes, through the fall and winter (*Rosenfield et al.,* 1994). After a few winter months of BDC-driven diabatic descent, the anomaly arrives in the Antarctic lower stratosphere in July-September, about 1 year after it formed in the middle tropical stratosphere (*Strahan et al.*, 2015). Continued descent and mixing across the polar tropopause bring the N_2O depleted air down to the surface ~4 months later, consistent with the long (17-19 month) delay between the QBO index at 20 hPa and the surface SH N_2O AGR anomalies in NOAA surface station data found in our analysis (Figure 6).

The strong isolation of the Antarctic polar vortex prevents mixing with midlatitudes during the period of diabatic descent from the altitude of the surf zone and is consistent with our finding that significant correlations with the NOAA surface N_2O AGR in the SH occur mainly for higher altitude QBO indices between about 30 and 10 hPa. The positive sign of the N_2O AGR correlation with the QBO index at those altitudes may be explained by the fact that the QBO meridional circulation brings less N_2O depleted air into the subtropical surf zone during the phase when the QBO is positive (westerly winds) in the upper tropical stratosphere above about 30 hPa (*Strahan et al.*, 2015). This leads to a positive N_2O anomaly (i.e., photochemically depleted, but less depleted than average) in the surf zone that ultimately is mixed into the polar region and transported into the troposphere via diabatic descent and mixing. When this signal of low N_2O depletion reaches the Earth's surface, it results in a more positive N_2O AGR than normal, hence the positive correlation with the positive (westerly) QBO at 10-30 hPa that originally drove the stratospheric N_2O anomaly well over one year earlier.

In the NH, some of the same mechanisms and interactions between the QBO and BDC occur, but they are more difficult to isolate than in the SH due to the larger wave activity in the NH compared to the SH (*Holton et al.*, 1995; *Scaife and James*, 2000, *Kidston et al.*, 2015). The deposition of momentum from planetary scale Rossby waves propagating into the stratosphere is the fundamental driver of the BDC. *Holton and Tan* (1980) originally showed that a deep and cold northern winter polar vortex was associated with the QBO westerly phase, and a weaker and warmer vortex associated with the easterly phase. Hence, the year-to-year integrated strength of the BDC is tied to the interaction of the NH mean flow with the QBO. Further, the BDC strength and structure is also tied to meridional mixing of air (*Shepherd*, 2007). In addition to the QBO influence on the northern polar vortex, the QBO induces a meridional circulation that directly impacts the northern mid-latitudes (e.g., *Randel and Wu*, 1996). The NH mid-winter QBO and wave mean-flow interaction has two effects: 1) it modulates the strength and structure of the BDC, and 2) it also modifies mixing between the Arctic polar vortex and the northern mid-latitudes by Rossby waves. These complex dynamics may explain why the N_2O AGR in the NH correlates best with lower stratosphere QBO indices, why the correlation has a negative rather than positive sign (due to the vertical reversal of the sign of QBO with altitude) and why the correlations is weaker than in the SH.

References

Baldwin, M.P., Gray, L.J., Dunkerton, T.J., Hamilton, K., Haynes, P.H., Randel, W.J., Holton, J.R., Alexander, M.J., Hirota, I., Horinouchi, T., Jones, D.B.A., Kinnersley, J.S., Marquardt, C., Sato, K., Takahashi, M.: The quasi-biennial oscillation, Reviews of Geophysics, 39(2), 179-229, 2001.

Carlin, B.P. and T.A. Louis, *Bayes and Empirical Bayes Methods for Data Analysis*, Chapman and Hall, New York, 2000.

Holton, J.R., Tan, H.C.: The Influence of the Equatorial Quasi-Biennial Oscillation on the Global Circulation at 50 mb, J. Atmos. Sci., 37, 2200-2208, DOI:https://doi.org/10.1175/1520-0469(1980)037<2200:TIOTEQ>2.0.CO;2, 1980.

Holton, J.R., Haynes, P.H., McIntyre, M.E., Douglass, A.R., Rood, R.B. and Pfister, L.: Stratosphere-troposphere exchange, Rev. Geophys., 33(4), 403-439, 1995.

Kidston, J., Scaife, A., Hardiman, S. et al.: Stratospheric influence on tropospheric jet streams, storm tracks and surface weather, Nature Geosci 8, 433–440, https://doi.org/10.1038/ngeo2424, 2015.

Prather, M. Hsu, J., J., DeLuca, N.M., Jackman, C.H., Oman, L.D., Douglass, A.R., Fleming, E.L., Strahan, S.E., Steenrod, S.D., Sovde, O.A., Isaksen, I.S.A., Froidevaux, L., Funke, B.: Measuring and modeling the lifetime of nitrous oxide including its variability, J. Geophys. Res. Atmos., 120, doi:10.1002/2015JD023267, 2015.

Randel, W. J., and Wu, F: Isolation of the ozone QBO in SAGE II data by singular decomposition, J. Atmos. Sci., 53, 2546–2559, 1996.

Rosenfield, J. E., P. A. Newman, and M. R. Schoeberl: Computations of diabatic descent in the stratospheric polar vortex, J. Geophys. Res., 99, 16,677–16,689, doi:10.1029/94JD01156, 1994.

Ruiz, D.J., Prather, M.J., Strahan, S.E., Thompson, R.L., Froidevaux, L., and Steenrod, S.D.: How atmospheric chemistry and transport drive surface variability of N_2O and CFC-11, J. Geophys. Res., 2021

Scaife, A.A. and James, I.N.: Response of the stratosphere to interannual variability of tropospheric planetary waves, Q.J.R. Meteorol. Soc., 126: 275- 297, https://doi.org/10.1002/qj.49712656214, 2000.

Shepherd, T. G.: Transport in the middle atmosphere, J. Meteorol. Soc. Jpn. Ser. II, 85, 165–191, 2007.

Sokal, R.R. and F.J. Rohlf, *Biometry*, 859 pp., W.H. Freeman, New York, 1981.

Strahan, S. E., Oman, L.D., Douglass, A.R. and Coy, L.: Modulation of Antarctic vortex composition by the quasi-biennial oscillation, Geophys. Res. Lett., 42, 4216–4223, doi:10.1002/2015GL063759, 2015.

Supplementary Figures S1-S3

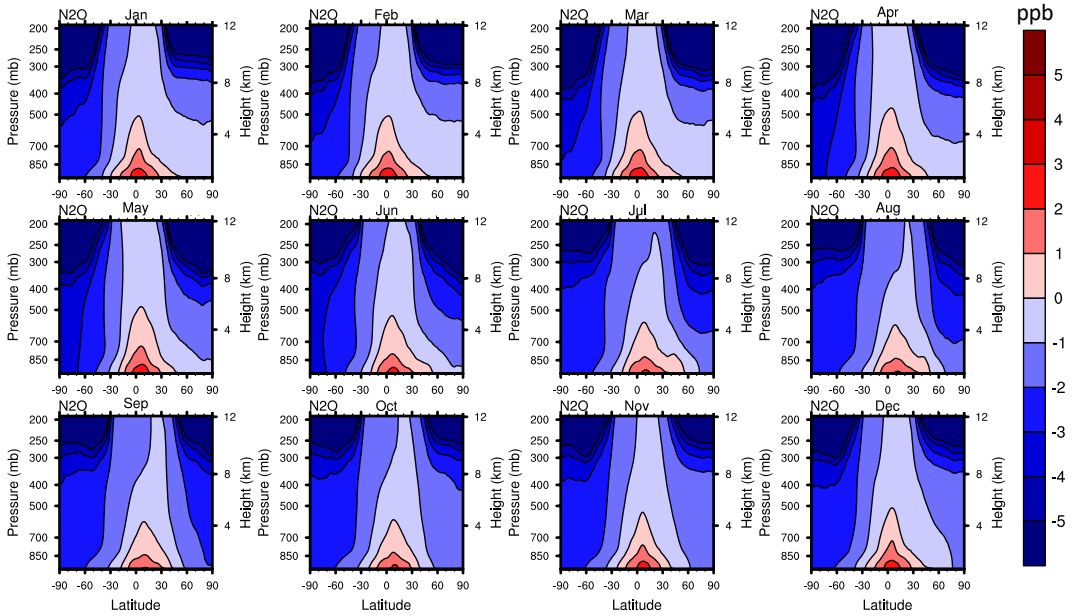

Figure S1: GEOSCCM monthly N_2O anomalies in ppb as a function of latitude and altitude extending from the surface up to 200 hPa (about 12 km). From left to right: January, February, March, April (top row); May, June, July, August (middle row); September, October, November, December (bottom row).

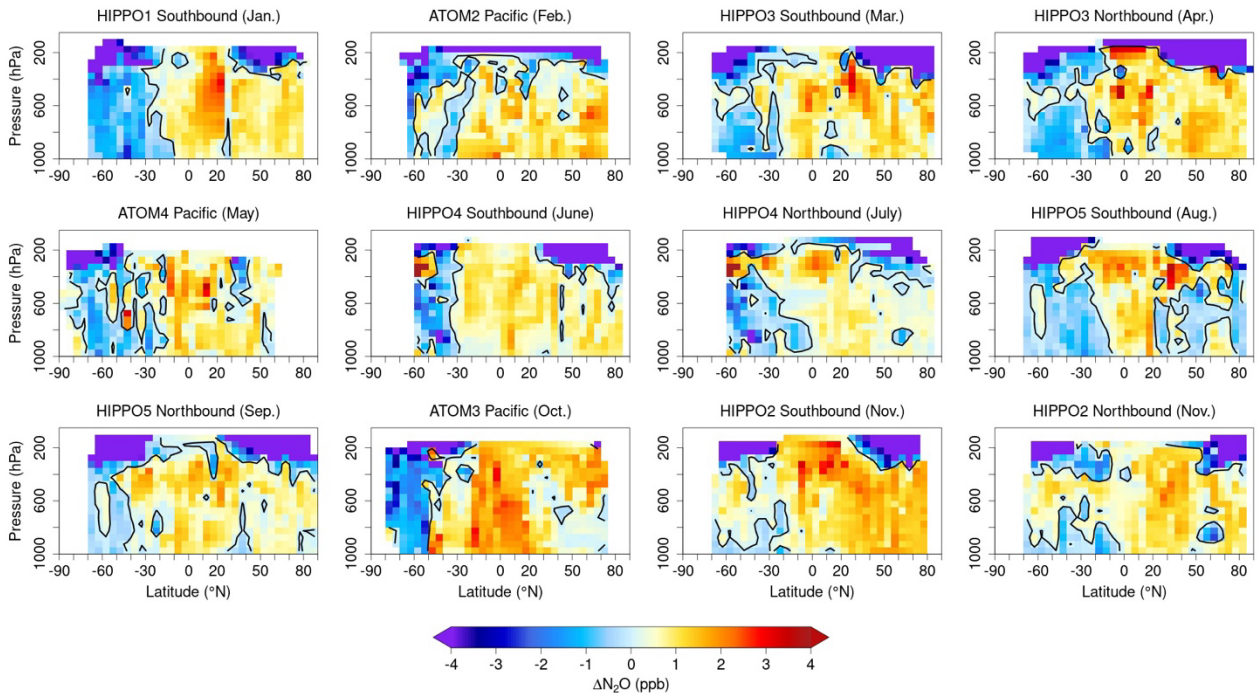

Figure S2: Similar to Figure 5 in the main text but including a larger collection of north and southbound HIPPO and ATom transects arranged to form an annual sequence. A deseasonalized fit to the NOAA time series at Mauna Loa has been subtracted to collapse all data to a single climatological year.

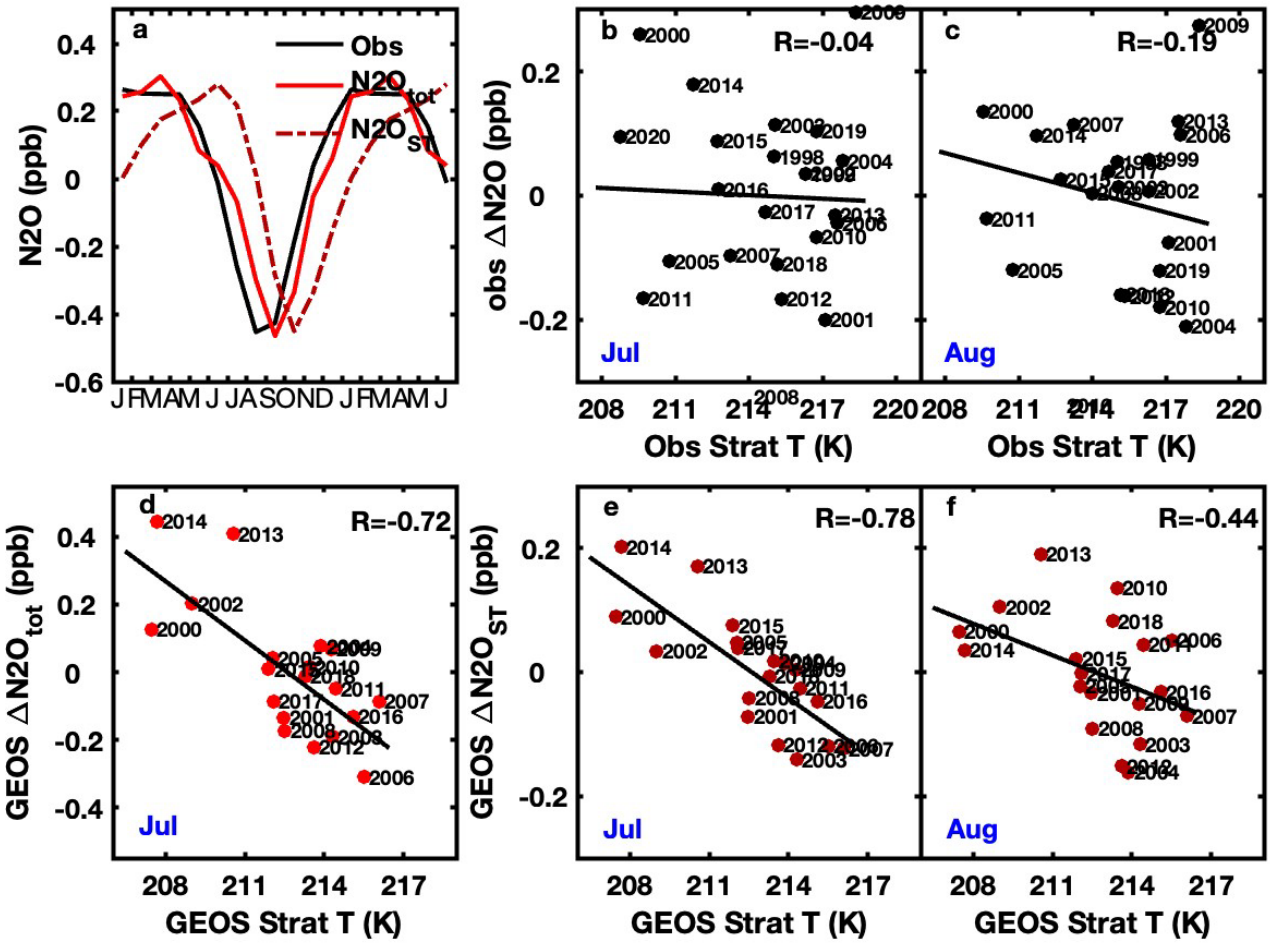

Figure S3: a) Mace Head, Ireland (MD) mean seasonal cycle in N_2O for NOAA observed N_2O and GEOSCCM total N_2O and N_2O_{ST}. NOAA surface N_2O seasonal anomalies in b) July and c) August for data spanning 1997-2021, plotted vs. mean lower stratospheric MERRA-2 temperature at 100 hPa averaged over 60-90°N over the previous winter (January-March). Bottom row shows GEOSCCM seasonal anomalies at MHD spanning 2000-2019 for d) total N_2O in July and N_2O_{ST} in e) July and f) August plotted vs. mean GEOS lower stratospheric temperature at 100 hPa averaged over 60-90°N over the previous winter. N_2O is descending into its seasonal minimum in July and August in the NH. (Note: while no correlation is found for NOAA July and August N_2O anomalies, significant correlations were found previously in AGAGE data (Nevison et al., 2011)).

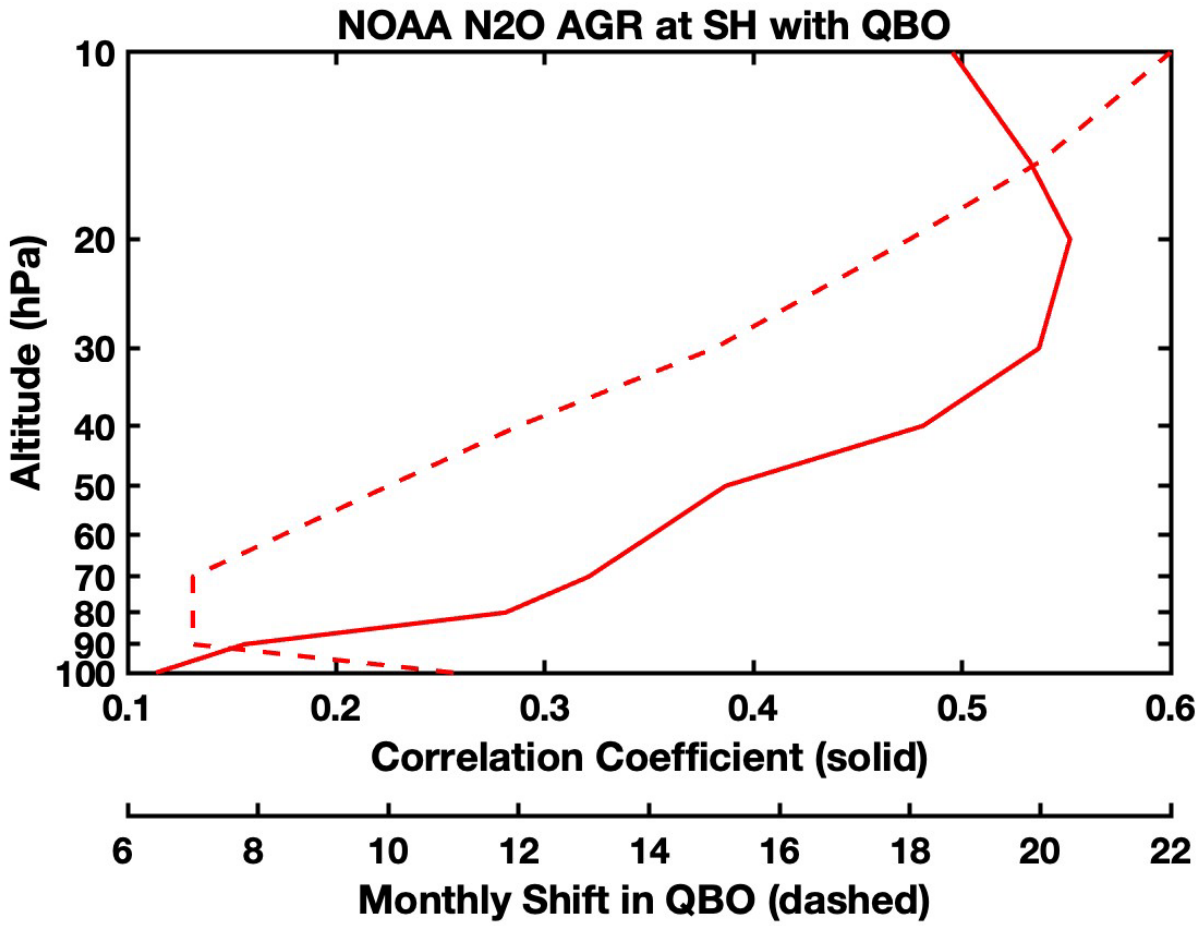

Figure S4: Southern Hemisphere N_2O atmospheric growth rate (AGR) for NOAA plotted vs. the QBO index ranging from 100 to 10 hPa with the optimal correlation coefficient (solid) and monthly forward shift in the index (dashed).